Preparations and Characterizations of Novel *N*, *N'*-Ethylene-Bridged-(*S*)-Histidyl-(*S*)-Tyrosine Derivatives and Their Copper(II) Complexes as Models of Galactose Oxidase

Kazuhiro Yamato, Takanori Inada, Matsumi Doe, Akio Ichimura, Takeji Takui, Yoshitane Kojima,* Toshimitsu Kikunaga,† Shin Nakamura,† Naohisa Yanagihara,† Tomoko Onaka,†† and Shigenobu Yano††

Department of Chemistry, Graduate School of Science, Osaka City University, Sugimoto, Sumiyoshi-ku, Osaka 558-8585

†Department of Materials Science, Faculty of Science and Engineering, Teikyo University, Toyosato-dai, Utsunomiya 320-8551

††Department of Chemistry, Faculty of Science, Nara Women's University, Kitauoyahigashi-machi, Nara 630-8506

(Received October 21, 1999)

Structurally constrained ethyl (2*S*)-3-(4-hydroxyphenyl)-2-{[(3*S*)-3-(imidazole-4-yl)-methyl]-2-oxo-piperazine-1-yl}propionate (*N*,*N'*-ethylene-bridged-(*S*)-histidyl-(*S*)-tyrosine ethyl ester, eHY–OEt) was obtained by a one-pot reaction from (*S*)-histidine methyl ester and (*S*)-tyrosine ethyl ester with glyoxal. Four ligands, (Boc–Gly–eHY–OEt (HL1), Boc–Gly–eHY–NH_2 (HL2), Ac–eHY–OEt (HL3), and Ac–eHY–NH_2 (HL4), where Boc–Gly is *t*-butyloxycarbonyl-glycyl and Ac is acetyl) were derived from eHY–OEt. Also, corresponding copper(II) complexes, in which only amino acid side chains coordinate to the copper(II) ion, $[Cu(L1^-)_2(H_2O)]$ **1**, $[Cu(L2^-)_2(H_2O)]$ **2**, $[Cu(L3^-)_2(H_2O)]$ **3**, and $[Cu(L4^-)_2(H_2O)]$ **4**, were prepared and characterized by elemental analyses and the FAB-MS spectra. The conformational behaviors were confirmed by the ^1H NMR spectra. UV-visible-NIR, CD and ESR spectra showed that copper(II) complexes are mononuclear square-pyramidal structures in both the solid and solution states. Cyclic voltammetry of HL1 and **1** showed irreversible ligand oxidation. The acid-dissociation constants of HL4 were obtained as 6.38 (pK_{a1}) and 9.67 (pK_{a2}) by potentiometric titration, and the complex formation constants of **4** were obtained as 7.16 ($\log K_1$) and 3.71 ($\log K_2$). Furthermore, thermogravimetric analyses (TGA) and differential thermal analyses (DTA) of **1** and **2** were measured.

Galactose oxidase (EC 1.1.3.9, GAO) is an extracellular copper enzyme which catalyzes the oxidation of D-galactose and low molecular weight primary alcohols to corresponding aldehydes (Eq. 1).[1] Though this enzyme contains one copper ion at its active site, it catalyzes two-electron oxidation:

$$R\text{–}CH_2OH + O_2 \rightarrow R\text{–}CHO + H_2O_2 \quad (1)$$

Knowles et al. have reported an X-ray crystal structure of GAO where a copper ion adopts a square-pyramidal geometry with two histidine imidazoles (His 496 and 581), two tyrosine phenolates (Tyr 272 and 495) and a fifth extragenous acetate (at pH 4.5) or water (at pH 7).[2] It was also revealed that tyrosine 272 is covalently linked at the *ortho* position of phenol by a thioether bond to the sulfur atom of cysteine 228. This novel organic cofactor exists in a phenoxyl radical and serves as a second oxidant.[3] Because of these characteristics, many model complexes have been reported for such targets: 1) phenoxyl radical,[4] 2) axial coordinate phenolate,[5] 3) thioether bound phenol,[6] 4) alcohol oxidation[7—9] and so on. Recently, Stack et al.[8] and Wieghardt et al.[9] reported functional model complexes that oxidized alcohol catalytically. However, the model complexes to which only amino acid side chains coordinate have been rarely reported,[10] because the peptides have low solubility to organic solvents and exist as a mixture of many conformational isomers in a solution. In order to resolve these problems, we have developed the chemistry of structurally constrained *N*,*N'*-ethylene-bridged-dipeptides.[11] Recently, we reported that *N*,*N'*-ethylene-bridged-(*S*)-histidyl-(*S*)-histidine methyl ester (eHH–OMe) derivatives could coordinate to copper(II) ions solely via nitrogen atoms of histidine imidazole,[12] such as hemocyanin[13] or superoxide dismutase.[14] Here, we report preparations of novel structurally constrained (2*S*)-3-(4-hydroxyphenyl)-2-{[(3*S*)-3-(imidazole-4-yl)-methyl]-2-oxo-piperazine-1-yl}propionic acid (*N*,*N'*-ethylene-bridged-(*S*)-histidyl-(*S*)-tyrosine, eHY) derivatives (Chart 1) and their copper(II) complexes as models of GAO.

Experimental

Materials and Methods. All chemicals were reagent grade. *t*-Butyloxycarbonyl-glycyl-*N*,*N'*-ethylene-bridged-(*S*)-histidyl-(*S*)-histidine methyl ester (Boc–Gly–eHH–OMe)[12] and *t*-butyloxycarbonyl-*N*,*N'*-ethylene-bridged-(*S*)-tyrosyl-(*S*)-tyrosine ethyl ester (Boc–eYY–OEt)[15] were prepared according to our previous method. ^1H NMR spectra were recorded on JEOL LA-400 and Varian U-500

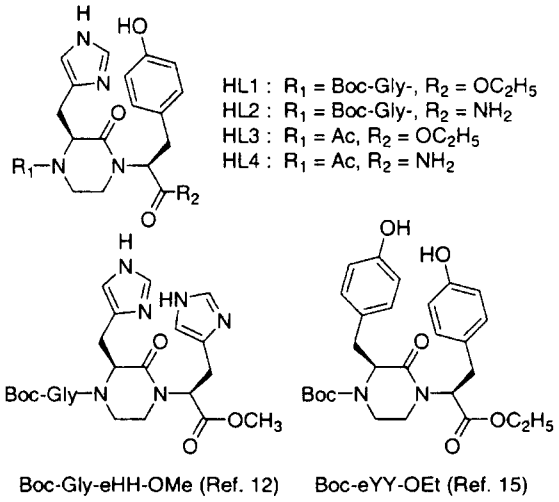

Chart 1.

FT-NMR spectrometers. Me_4Si was used as an internal standard in a $CDCl_3$ solution. In the case of DMSO-d_6, a residual solvent peak was used as an internal standard. IR spectra were obtained on a JASCO FT/IR-420 spectrometer. Melting points were determined on a Yanaco MP-J3 apparatus. Specific rotations $[\alpha]_D$ were taken on a JASCO DIP 300 polarimeter. Mass spectra were recorded on a JEOL AX-500 mass spectrometer. UV-visible-NIR spectra were recorded on a Hitachi U-3500L spectrophotometer. CD spectra were taken on JASCO J-720 and J-730 spectropolarimeters.

Ethyl (2*S*)-3-(4-Hydroxyphenyl)-2-{[(3*S*)-3-(imidazole-4-yl)-methyl]-2-oxo-piperazine-1-yl}propionate (*N*,*N*′-Ethylene-bridged-(*S*)-histidyl-(*S*)-tyrosine Ethyl Ester, eHY–OEt) and *N*-[(2*S*)-3-(Imidazole-4-yl)-1-methoxy-1-oxo-propane-2-yl]-*N*′-[(2*S*)-3-(4-hydroxyphenyl)-1- ethoxy-1-oxo-propane-2-yl]-ethylenediamine (*N*,*N*′-Ethylene-[(*S*)-histidine Methyl Ester]-[(*S*)-tyrosine Ethyl Ester], MeO–HeY–OEt). After a methanol solution of (*S*)-tyrosine ethyl ester hydrochloride (9.87 g, 20 mmol) and 40% glyoxal aqueous solution (4.41 g, 30 mmol) was stirred for 2 h at 0 °C, (*S*)-histidine methyl ester dihydrochloride (4.87 g, 20 mmol) and triethylamine (2.03 g, 20 mmol) were added. After 1 h, sodium cyanotrihydroborate (3.79 g, 60 mmol) was added and the reaction was stirred overnight at room temperature. A white precipitate was removed by filtration, and the filtrate was evaporated. Two products were isolated by basic silica-gel column chromatography (Fuji Silysia NH-DM1020, $CHCl_3$–CH_3OH) and an acidic one (Fuji Silysia BW-820MH, $CHCl_3$–CH_3OH). Further purification was achieved by gel filtration (Sephadex LH-20, CH_3OH).

eHY–OEt; Yield: 20%. Mp 86—90 °C. Anal. Calcd for $C_{19}H_{24}N_4O_4 \cdot 1.4H_2O$ (Hygroscopic): C, 57.39; H, 6.79; N, 14.09%. Found: C, 57.95; H, 6.70; N, 13.72%. ^1H NMR ($CDCl_3$): δ = 7.40 (s, 1H), 6.96 (d, 2H), 6.75 (d, 2H), 6.56 (s, 1H), 5.27 (dd, 1H), 4.21 (m, 2H), 3.69 (t, 1H), 3.29 (dd, 1H), 3.21 (ddd, 1H), 3.06 (m, 2H), 2.91 (m, 5H), 1.28 (t, 3H). IR ($CHCl_3$) $\nu_{C=O}$ = 1730 and 1635 cm^{-1}. $[\alpha]_D = -155.7$ deg dm^{-1} cm^3 (CH_3OH). FAB MS *m/z* 373 ($[M+H]^+$).

MeO–HeY–OEt: Yield: 20%. Mp 32—36 °C. Anal. Calcd for $C_{20}H_{28}N_4O_5 \cdot 0.8H_2O$ (Hygroscopic): C, 57.35; H, 7.12; N, 13.38%. Found: C, 57.37; H, 7.02; N, 13.31%. ^1H NMR ($CDCl_3$) δ = 7.39 (s, 1H), 6.98 (d, 2H), 6.78 (d, 2H), 6.71 (s, 1H), 4.15 (q, 2H), 3.68 (s, 3H), 3.48 (m, 2H), 2.95 (m, 2H), 2.80 (m, 4H), 2.50 (d, 2H), 1.23 (t, 3H). IR ($CHCl_3$) $\nu_{C=O}$ = 1730 cm^{-1}. $[\alpha]_D = +4.8$ deg dm^{-1} cm^3 (CH_3OH). FAB MS *m/z* 405 ($[M+H]^+$).

Cyclization of MeO–HeY–OEt to eHY–OEt. MeO–HeY–OEt was kept for several days at 40 °C. The reaction was monitored by the IR spectrum. Finally, eHY–OEt was quantitatively obtained.

Boc–Gly–eHY–OEt (HL1). A dichloromethane solution of eHY–OEt (650 mg, 1.75 mmol) and *t*-butyloxycarbonyl-glycine *N*-hydroxysuccinimide ester (Boc–Gly–OSu) (717 mg, 2.63 mmol) was stirred for 12 h. After removing of the solvent, the oily residue was purified by column chromatography (NH-DM1020, $CHCl_3$–CH_3OH). Yield: 76%. Mp 117—123 °C. Anal. Calcd for $C_{26}H_{35}N_5O_7 \cdot 3/4H_2O$ (Hygroscopic): C, 57.50; H, 6.77; N, 12.89%. Found: C, 57.37; H, 6.80; N, 12.89%. IR ($CHCl_3$) $\nu_{C=O}$ = 1735, 1707 (sh), and 1647 cm^{-1}. $[\alpha]_D = -12.1$ deg dm^{-1} cm^3 (CH_3OH). FAB MS *m/z* 530 ($[M+H]^+$).

Ac–eHY–OEt (HL3). This compound was prepared by the similar method as that mentioned above, except for using acetic acid *N*-hydroxysuccinimide ester (Ac–OSu) in place of Boc–Gly–OSu. Yield: 73%. Mp 111—115 °C. Anal. Calcd for $C_{21}H_{26}N_4O_5 \cdot 1.6H_2O$ (Hygroscopic): C, 56.90; H, 6.64; N, 12.64%. Found: C, 57.08; H, 6.32; N, 12.52%. IR ($CHCl_3$) $\nu_{C=O}$ = 1730, 1655 (sh), and 1635 cm^{-1}. $[\alpha]_D = -43.3$ deg dm^{-1} cm^3 (CH_3OH). FAB MS *m/z* 415 ($[M+H]^+$).

Boc–Gly–eHY–NH_2 (HL2). This compound was quantitatively obtained by blowing NH_3 gas into the methanol solution of HL1. Mp 160—168 °C. Anal. Calcd for $C_{24}H_{32}N_6O_6 \cdot 1.8H_2O$ (Hygroscopic): C, 54.90; H, 6.37; N, 15.77%. Found: C, 54.77; H, 6.77; N, 15.55%. IR ($CHCl_3$) $\nu_{C=O}$ = 1694 and 1650 cm^{-1}. $[\alpha]_D = +15.1$ deg dm^{-1} cm^3 (CH_3OH). FAB MS *m/z* 501 ($[M+H]^+$).

Ac–Gly–eHY–NH_2 (HL4). This compound was prepared by the same method as that mentioned above, except for using HL3 in place of HL1. Mp. 150—154 °C. Anal. Calcd for $C_{19}H_{23}N_5O_4 \cdot 1.4H_2O$ (Hygroscopic): C, 55.57; H, 6.33; N, 17.05%. Found: C, 55.55; H, 6.38; N, 17.05%. IR ($CHCl_3$) $\nu_{C=O}$ = 1685 and 1630 cm^{-1}. $[\alpha]_D = -5.4$ deg dm^{-1} cm^3 (CH_3OH). FAB MS *m/z* 386 ($[M+H]^+$).

$[Cu(L1^-)_2(H_2O)] \cdot H_2O$ (1). After $CuCl_2 \cdot 2H_2O$ (41 mg, 0.24 mmol) was added to 20 cm^3 of a methanol solution of HL1 (250 mg, 0.47 mmol) and sodium methoxide (26mg, 0.47 mmol), the mixture was stirred for 12 h at room temperature. After removing of the solvent, the residue was recrystallized from dichloromethane–hexane. Yield: 57%. Mp 157—161 °C (decomp). Anal. Calcd for $Cu(C_{26}H_{34}N_5O_7)_2 \cdot 2H_2O$: C, 53.97; H, 6.27; N, 12.11%. Found: C, 54.16; H, 6.26; N, 12.15%. IR (KBr) $\nu_{C=O}$ = 1735, 1701, and 1649 cm^{-1}. $[\alpha]_D = +0.75$ deg dm^{-1} cm^3 (CH_3OH). FAB MS *m/z* 1120 ($[M-H_2O+H]^+$).

Other copper complexes (**2**—**4**) were prepared by the same method as that of **1**, except for the condition of recrystalization.

$[Cu(L2^-)_2(H_2O)] \cdot 2.5H_2O$ (2). **2** was recrystallized from ethanol. Yield: 29%. Mp 183—189 °C (decomp). Anal. Calcd for $Cu(C_{24}H_{31}N_6O_6)_2 \cdot 4.5H_2O$: C, 50.48; H, 6.52; N, 14.15%. Found: C, 50.81; H, 6.29; N, 13.98%. IR (KBr) $\nu_{C=O}$ = 1675 and 1647 cm^{-1}. $[\alpha]_D = -62$ deg dm^{-1} cm^3 (CH_3OH). FAB MS *m/z* 1062 ($[M-H_2O+H]^+$).

$[Cu(L3^-)_2(H_2O)] \cdot 3H_2O$ (3). **3** was recrystallized from ethanol.[16] Yield: 12%. Mp 170—175 °C (decomp). Anal. Calcd for $Cu(C_{21}H_{25}N_4O_5)_2 \cdot 4H_2O$: C, 52.41; H, 6.07; N, 11.64%. Found: C, 52.63; H, 6.08; N, 11.43%. IR (KBr) $\nu_{C=O}$ = 1735 and 1637 cm^{-1}. $[\alpha]_D = -208$ deg dm^{-1} cm^3 (CH_3OH). FAB MS *m/z* 890 ($[M-H_2O+H]^+$).

$[Cu(L4^-)_2(H_2O)] \cdot 1.5H_2O$ (4). **4** was recrystallized from methanol.[16] Yield: 4%. Mp 176—180 °C (decomp). Anal. Calcd for $Cu(C_{19}H_{22}N_5O_6)_2 \cdot 2.5H_2O$: C, 47.62; H, 6.10; N, 14.62%. Found: C, 48.21; H, 5.71; N, 14.13%. IR ($CDCl_3$) $\nu_{C=O}$ = 1675

and 1633 cm^{-1}. $[\alpha]_D = -126$ deg dm^{-1} cm^3 (CH_3OH). The FAB MS spectrum was not obtained because of low solubility.

ESR Spectra. X-band ESR spectra were taken on a Bruker ESP 300 spectrometer equipped with a TM mode microwave cavity. The temperature at the sample side was controlled by a liquid-nitrogen gas controller. A simulation for randomly oriented ESR spectra was performed by software (Scimphonia) based on the second-order perturbation theory. No resolution of the ^{63}Cu and ^{65}Cu lines was obtained in the experiment. Thus, the spectral simulation did not include distinction of the two nuclei.

Cyclic Voltammetry (CV). Acetonitrile (Nacalai Tesque) was distilled over CaH_2. Tetrabutylammonium hexafluorophosphate (Bu_4NPF_6) was prepared by the metathesis of Bu_4NBr and KPF_6, washed thoroughly with water, recrystallized three times from ethanol, and dried under reduced pressure at 80 °C.[17] CV measurements were performed with a BAS CV-50W voltammetric analyzer. The working electrode was a glassy carbon disk (3 mm diameter), which was polished with a 0.3 μm alumina slurry before each voltammetric run. The reference electrode was an Ag/$AgPF_6$ (1.0×10^{-3} mol dm^{-3}), Bu_4NPF_6 (0.1 mol dm^{-3}) in CH_3CN, against which the formal potential ($E^{\circ\prime}$) of a ferrocene/ferrocenium couple was +63 mV. The measured potential values (vs. Ag/$AgPF_6$) were converted to those vs. NHE by adding +337 mV based on E° ferrocene/ferrocenuium (+400 mV vs. NHE). The voltammetric studies were recorded in CH_3CN with 0.1 mol dm^{-3} Bu_4NPF_6 as a supporting electrolyte. All solutions were purged with pure Ar in order to remove any dissolved O_2 and were maintained at 25 °C.

Potentiometric Measurements. All potentiometric titrations were performed in a double-walled titration cell with a capacity of 100 cm^3, and all hydrogen-ion concentrations were determined by a Toa Electronics Ltd. IM 40S ion meter. The temperature of the solutions was maintained at 25.0 ± 0.05 °C by circulating thermostated water through the outer jacket of the cell. A pH combination electrode was calibrated using commercially available buffer solution standards (4.01, 6.86 and 9.18). The ionic strength (μ) of the experimental solutions was maintained at 0.1 mol dm^{-3} by the addition of an appropriate amount of 1.0 mol dm^{-3} potassium nitrate. The ion product of water at 25.0 °C in potassium nitrate media was taken to be the same as that in a previously reported method.[18] The solutions were stirred with a magnetic stirrer and bubbled by nitrogen gas; a positive nitrogen pressure was maintained during all experiments in order to prevent contamination of the atmosphere. In this study, the pH is defined as the logarithm of the concentration, $(-\log [H^+])$, instead of the generally used hydrogen-ion activity function. The concentrations of the reactants in the experimental solutions were of the order of $2.0—5.0\times10^{-3}$ mol dm^{-3} for each component.

The acid dissociation constants of HL4 and the stability constants of the copper(II) complexes with HL4 were directly obtained by potentiometric data using the computer programs PKAS (pK_a) and BEST ($\log K$).[19]

Thermal Analyses. A thermogravimetric analysis (TGA) and a differential thermal analysis (DTA) were determined on a Shimadzu DT-40. Small portions (ca. 10—15 mg) of the complexes were used for these analyses, and highly sintered α-Al_2O_3 was the thermally inert reference material for the DTA measurements. TG and DTA curves were recorded upon being heated up to 650 °C at a rate of 5 °C min^{-1} in a dynamic atmosphere of nitrogen at a rate of 20 cm^3 min^{-1}.

Results and Discussion

Syntheses of Ligands and Copper(II) Complexes. The syntheses of the ligands are summarized in Scheme 1. A one-pot reaction of (*S*)-tyrosine ethyl ester and (*S*)-histidine methyl ester with glyoxal in the presence of sodium cyanotrihydroborate gave *N*,*N*′-ethylene-bridged-(*S*)-histidyl-(*S*)-tyrosine ethyl ester (eHY–OEt) and *N*,*N*′-ethylene-[(*S*)-histidine methyl ester]-[(*S*)-tyrosine ethyl ester] (MeO–HeY–OEt). Furthermore, MeO–HeY–OEt was easily converted to eHY–OEt by standing at 40 °C for several days without the formation of *N*,*N*′-ethylene-bridged-(*S*)-tyrosyl-(*S*)-histidine methyl ester (eYH–OMe). As a result, the total yield of eHY–OEt was higher than 40%. Protection of the terminal imino nitrogen was achieved by standard peptide syntheses with two kinds of activated *N*-hydroxy succinimide esters: *t*-butyloxycarbonyl-glycyl (HL1) and acetyl (HL3), to control hydrophobicity. The corresponding amide derivatives (HL2 and HL4) were obtained quantitatively by ammonia gas blowing.

The copper(II) complexes were obtained using complexation reactions between the appropriate ligands and $CuCl_2\cdot2H_2O$ in the presence of sodium methoxide. These complexes were characterized by CHN analyses, FAB MS spectra and IR spectra.

NMR Study of the Ligands. As shown in Fig. 1, for all four ligands there exist *cis*–*trans* conformers based on peptide-bond conformation of the *N*-terminal of the piperazine-2-one ring in the solution.[20] These behaviors were confirmed by the ^1H NMR spectra. For HL1, two signals of an α-methine proton (H_α) of histidine were observed at $\delta = 4.36$ (*cis*) and 4.96 (*trans*) in a $CDCl_3$ solution. In the 2D NOESY spectrum, a cross peak was observed arising from the chemical exchange between these two signals. A low magnetic shift of the H_α-proton of histidine can be reasonably explained by the fact that the α-proton is quasi-equatorial and is parallel to the C=O of a glycine peptide bond so that it is affected by the magnetic anisotropy of the acetyl carbonyl group.[20] Similarly, at the pseudo equatorial proton (H_{eq}) of a piperazine methylene group adjacent to the amide nitrogen of histidine, the peak of *cis* conformer was observed at a lower magnetic field; however, the peak overlapped with others. Furthermore, the relative ratio of the *cis*- and *trans*-conformers was estimated to be 1 : 1.3 based on the peak-integration values. Three other ligands behave in similar manners as HL1; the results of four ligands are summarized in Table 1. These results also show that the *cis*–*trans* equilibrium lies to *trans*-conformers.

UV-visible-NIR and CD Spectra. Figure 2 shows continuous variation plots (Job's plot) of $CuCl_2\cdot2H_2O$ and NaL1, which was generated in situ by mixing HL1 and sodium methoxide, in the visible region. In the 600—650 nm region, the maximum absorbance value is observed at $[Cu^{2+}]/\{[Cu^{2+}]+[L1^-]\} = 0.33$. These results suggest that the 2 : 1 ($L1^-$: copper) complex is predominantly formed in the solution.

Table 2 gives the maximum peaks of the electronic spectra of **1**—**3** in various solutions. In each solution, strong bands (400—450 nm) and broad weak bands (600—850 nm) are observed. In addition, the powder reflection spectrum of **1**

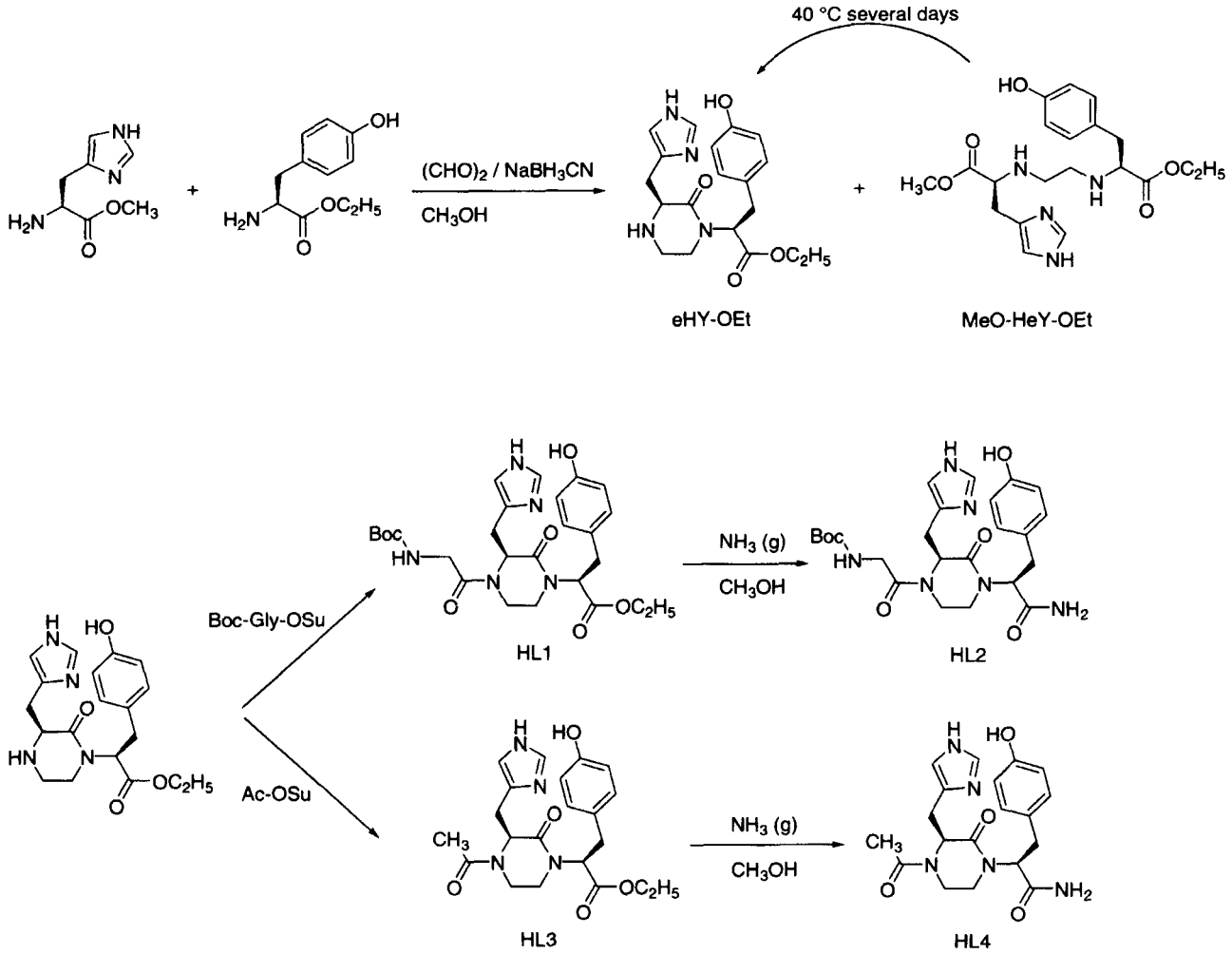

Scheme 1.

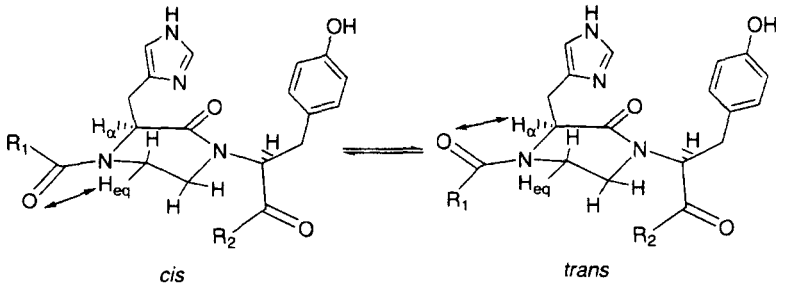

Fig. 1. Two conformers of the ligands in the solution.

contains the same features as those of the solutions. These two bands are assigned as ligands to a metal charge transfer (LMCT) of phenolate anions to copper ion for a strong band and d–d transition of copper ion for a broad weak band. Moreover, the CD spectra revealed that the d–d band consists of two overlapped components. These results suggest that the copper(II) ion exists in a square-pyramidal geometry.[21,22] The two components are assigned as d_{xz}, $d_{yz} \rightarrow d_{x^2-y^2}$, and d_{z^2}, $d_{xy} \rightarrow d_{x^2-y^2}$. Furthermore, these CD patterns resemble those of the inactive form of GAO (copper(II)-phenolate anion moiety).[23]

Itoh et al. and Whittaker et al. reported that phenolate bridged copper(II) dimer complexes are changed to monomer ones in solution by the addition of an excess amount of external ligand, like pyridine.[6] Figure 3 shows the UV-visible-NIR and CD spectra of **1** with or without 10 mole equivalent of pyridine in CH_3OH (solid line: without pyridine, dot-dash line: with pyridine) or CH_3CN (dashed line: without pyridine, dot line: with pyridine). In the 300—1100 nm region, no spectral change was observed by an addition of excess amount of pyridine. From the above results, it is suggested that complex **1** is a square-pyramidal monomer complex with

Table 1. Selected ^{1}H NMR Peaks and *cis–trans* Relative Ratios at Room Temperature

Ligand	Solvent	δ				Relative ratio
		H_α		H_{eq}		
		cis	*trans*	*cis*	*trans*	*cis* : *trans*
HL1	$CDCl_3$	4.36	4.96	a)	a)	1 : 1.3
HL2	DMSO-d_6	4.30	4.69	a)	a)	1 : 1
HL3	$CDCl_3$	4.41	4.98	4.32	3.52	1 : 1.5
HL4	DMSO-d_6	4.26	4.77	4.15	3.48	1 : 1.6

a) Signals are overlapped.

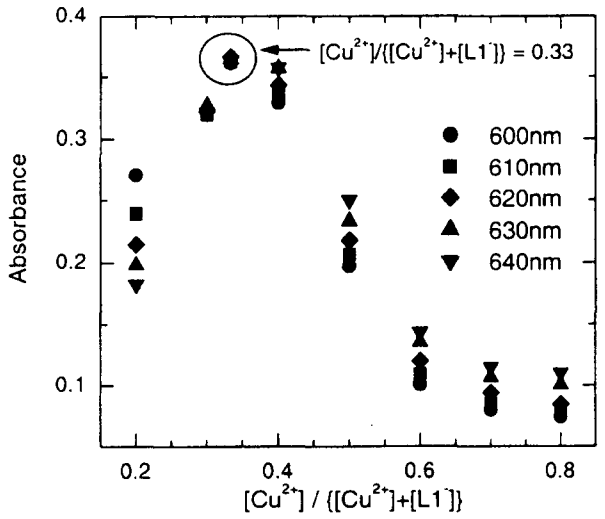

Fig. 2. Job's plot of $CuCl_2$ and NaL1 in CH_3OH at room temperature. $[Cu^{2+}]+[L1^-] = 1.5$ mmol dm^{-3}.

two imidazole nitrogen atoms, two phenolate oxygen atoms and one external water or solvent molecule (Fig. 4).[24]

Complexes **2** and **3** also have two-component d–d bands at similar regions, which suggests the square-pyramidal geometry. However, the Cotton patterns are different from those of **1**. These results may result from the conformations of the ligands and/or the positions of the coordinated atoms. However, the details are unclear.

ESR Spectra. An X-band ESR spectrum of **1** in a frozen glass of CH_3CN at 170 K showed a dominant axial character of the ligand environment with a small amount of rhombic distortion ($g_\parallel = 2.27$, $g_\perp = 2.04$, and $A_\parallel = 14.3$ mT, $A_\perp = 1.0$ mT), as shown in Fig. 5. Superhyperfine splittings attributed based on ^{14}N nuclei ($A_{N\parallel} = 1.4$ mT and $A_{N\perp} = 1.6$ mT) were also detected, and the 5-line splittings were resolved only at the g perpendicular region, suggesting that the imidazole nitrogen atoms coordinate to the Cu(II) center equivalently. The observed axial g values are characteristic of a Cu(II) ion in square-pyramidal coordination symmetry, which stabilizes a $d_{x^2-y^2}$ orbital ground state. These results are consistent with the mononuclear square-pyramidal structure of **1** proposed in the previous section. Taking into account the UV-vis-NIR and CD spectra of **1**, it is suggested that two ligand $L1^-$ coordinate equivalently on the equatorial plane, and that a water or solvent molecule occupies at the axial position. From the experimentally determined $g_\parallel$ and $g_\perp$ values, the molecular-orbital coefficients of 3d orbitals for $\Psi(b_{2g})$ and $\Psi(e_{2g})$ were evaluated to be $\beta_2 = 0.910$ and $\varepsilon = 0.633$, respectively, where the values for $\Delta_\parallel = E(B_{1g}) - E(B_{2g})$ and $\Delta_\perp = E(B_{1g}) - E(E_g)$ were obtained from the CD spectrum of complex **1** in CH_3CN; $\Delta_\parallel = 1.66\times10^4$ cm^{-3}, $\Delta_\perp = 1.29\times10^4$ cm^{-3}. The estimated values for β_2 and ε imply that a small amount of in-plane π bonding and quite a strong out-of-plane π bonding are taking place in complex **1**. It should be noted that the strong π bonding derived from the reduced values for ε is invalidated because the above analysis neglects the appreciable amount of rhombicity derived from the ESR data.

Moreover, a broad spectrum of **1** in CH_3CN was obtained at room temperature. This indicates that the ligand exchange or replacement occurs in the solution state, such as *cis–trans*

Table 2. Maximum Values of UV-visible-NIR and CD Spectra of **1**—**3** in Various Solvent and Powder

Complex	UV-visible spectra		CD spectra		
	λ_{max}/nm (ε/dm^3 mol^{-1} cm^{-1})		λ_{max}/nm ($\Delta\varepsilon$/dm^3 mol^{-1} cm^{-1})		
Solvent	LMCT	d–d	LMCT	d–d	
1 CH_3OH	403	606[a]	389	602	763
	(1940)	(169)	(−0.72)	(−0.21)	(+0.54)
1 CH_3CH	414	617[a]	389	602	763
	(1470)	(138)	(−0.88)	(−0.05)	(+0.60)
1 CH_2Cl_2	435	632[a]	430	632	813
	(1675)	(147)	(−0.84)	(−0.34)	(+0.89)
1 DMSO	415	671[a]	408	602	775
	(938)	(147)	(−0.71)	(−0.05)	(+0.55)
2 CH_3OH	397	621[a]	390	610	720
	(2210)	(127)	(−1.44)	(+0.42)	(+0.61)
3 CH_3OH	398	626[a]	390	620	732
	(1060)	(125)	(−0.96)	(+0.26)	(0.46)
1 Powder	410	617[a]			
GAO inactive from H_2O [b]	450	629	420	620	800

a) Shoulder. b) Refer to Ref. 23.

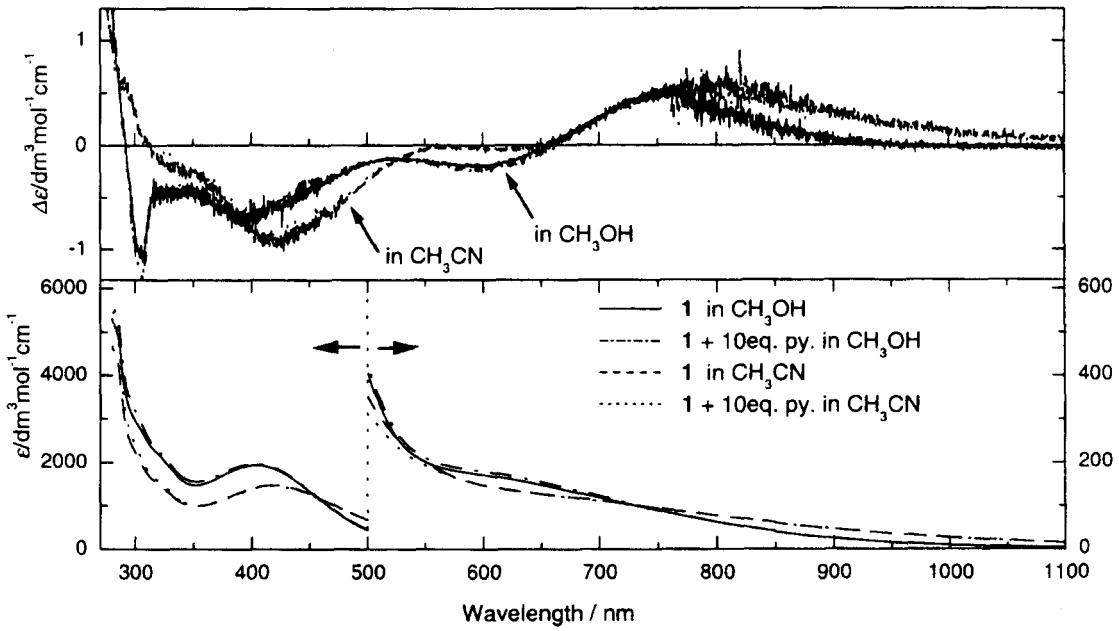

Fig. 3. UV-visible-NIR (lower) and CD (upper) spectral changes observed in addition of 10 mole equiv pyridine to **1** in CH_3OH or CH_3CN at room temperature. [**1**] = 1 mol dm^{-3}.

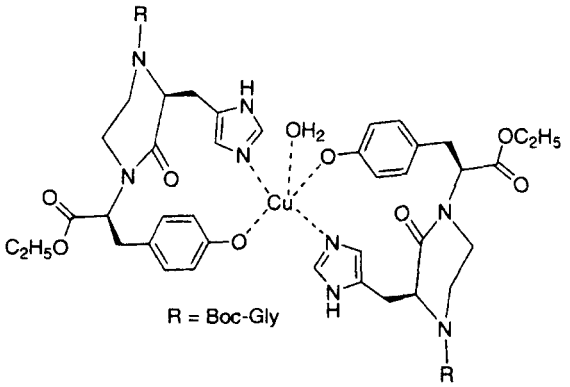

Fig. 4. Proposed structure of **1**.

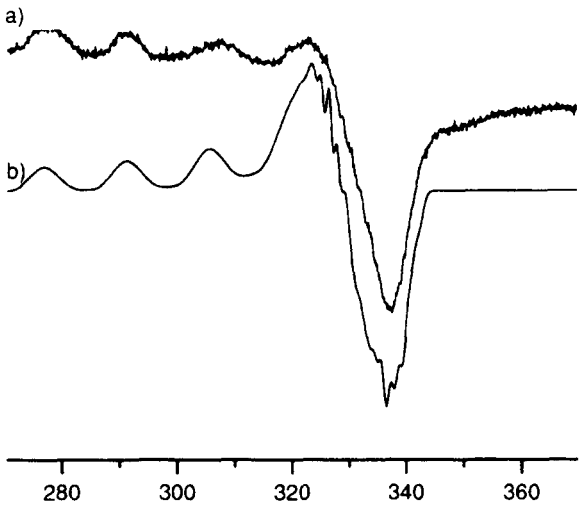

Fig. 5. a) ESR spectrum of **1** in CH_3CN glass at 170 K, microwave frequency 9.481586 GHz; modulation frequency 100 kHz; modulation amplitude 0.4014 mT; microwave power 1.00 mW. b) Simulated spectrum.

or an axial-equatorial rearrangement of the ligand and/or association–dissociation of coordinated water and the solvent molecule. The obtained isotropic parameters ($g_0 = 2.11$, $A_0 = 5.0$ mT) were consistent with those obtained from the powder-pattern ESR spectrurm in CH_3CN glass at low temperature.

Cyclic Voltammetry. Cyclic voltammograms of complex **1** (1×10^{-3} mol dm^{-3}) and its corresponding ligand HL1 (1×10^{-3} mol dm^{-3}) in CH_3CN containing 0.1 mol dm^{-3} of Bu_4NPF_6 on a glassy carbon electrode are shown in Figure 6. A positive scan (initiated at +337 mV (vs. NHE) for the ligand solution) gave two oxidation peaks with almost the same peak current at +870 mV (vs. NHE) and +1360 mV (vs. NHE), respectively. No peaks corresponding to the reduction appear on the reverse scan. By comparing of the voltammetric behavior for the oxidation of Boc–Gly–eHH–OMe (+1350 mV vs. NHE) and Boc–eYY–OEt (+1480 mV vs. NHE), the first and second oxidation processes are assigned to the oxidation of phenol and imidazole moieties, respectively. However, the first value is lower than that of the phenol group and the second one is higher than that of the imidazole moiety. It is known that the oxidation potentials of phenols decrease at a high pH value.[25] Thus, we assigned that the ligand exists as a zwitter ion form in solution, i.e., a phenolate anion-imidazolium cation. In other words, it is easily assumed that the oxidation potentials of the phenolate anion and imidazole (base) are lower than the corresponding phenol and imidazolium cation (conjugate acid), respectively.

Complex **1** exhibits a chemically irreversible and broad oxidation peak at +1540 mV (vs. NHE). The peak current is

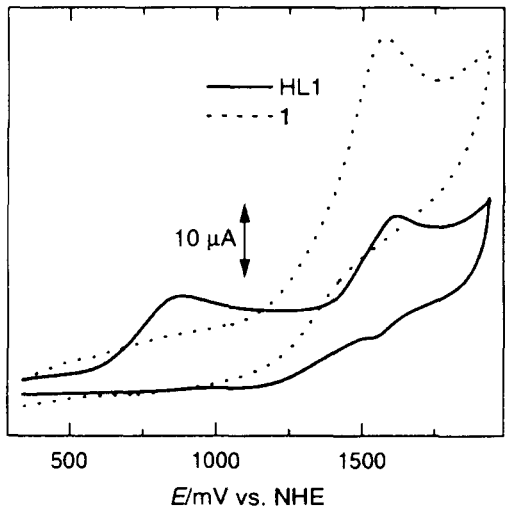

Fig. 6. Cyclic voltammograms of HL1 (solid line) and **1** (dashed line) in CH_3CN at room temperature.

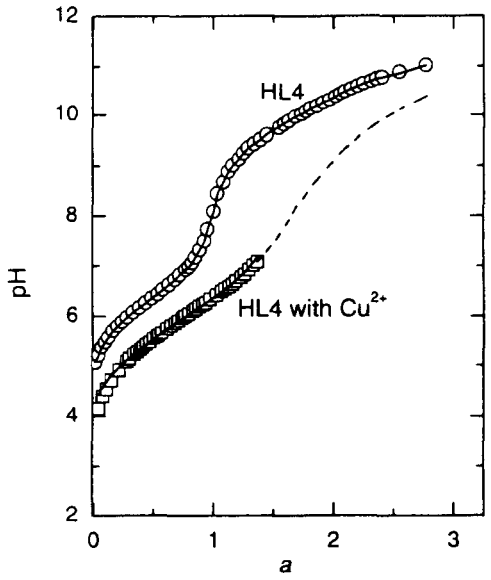

Fig. 7. Potentiometric titration curve for HL4 (○) and its copper complex (□): $t = 25.0$ °C, $\mu = 0.10$ mol dm^{-3} (KNO_3), and a = moles of base added per mole of ligand.

about two-times that for ligand HL1. These results indicate that the oxidation of **1** occurs on the ligand, probably phenolate moieties, rather than at the copper(II) center. This value is extremely higher than those of native GAO (+410 mV vs. NHE)[26] and other model complexes (+750—1000 mV vs. NHE).[4,6,8] In GAO and other model systems, electron-donating substituents, such as thioether, methoxy and *t*-butyl groups at *ortho*- and *para*-positions depress the oxidation potential and stabilize the phenoxyl radical. Furthermore, in GAO π–π stacking between tyrosine 272 and tryptophan 290 also stabilizes the phenoxyl radical.[2c,27] In contrast, no substituent groups at the *ortho*-positions of $L1^-$ cause a high oxidation potential. Also, the irreversibility can be reasonably explained by radical–radical coupling via the *ortho* position of the phenol ring.[28] No reduction process was observed within the accessible negative potential range, also indicating that the copper(II) state of **1** is extremely stable thermodynamically. The CV of complexes **2**—**4** were not measured because of no solubility in CH_3CN.

Potentiometric Measurements. The acid-dissociation constants of the ligand and the stability constants of the copper(II) complex were determined by potentiometric titration. Since the Boc group decomposes under an acidic condition and ester is hydrolyzed by the hydroxide ion, ligand HL4 was selected for these experiments. A potentiometric titration curve for ligand HL4 is shown in Fig. 7. The free-ligand curve first has a low-pH buffer zone and then an inflection point that is slightly higher than $a = 1$, where a represents the number of moles of NaOH added per mole of ligand. Following the inflection point, there is a long buffer region at high pH. Using PKAS,[19] the acid-dissociation constants were found to be pK_{a1} and $pK_{a2} = 6.38 \pm 0.01$ and 9.67 ± 0.01, respectively. The experimental data points (open circles) are in accord with the calculated values (solid line) that were obtained from the pK_a values.

Since the order of dissociation is ambiguous, (taking into account the possibility that only two substituent moieties, i.e., imidazolium cation with proton addition and phenol hydrogen, contribute to the acid dissociation processes), the assignment of the pK_a values was determined by comparing them with those of analogous compounds.[29,30] Subsequently, it is reasonable to conclude that the first dissociation constant is attributable to an imidazolium cation. The imidazolium cation dissociation constant ($pK_{a1} = 6.38$) is somewhat higher than the value for the imidazole ($pK_a = 6.02$) of (*S*)-histidine.[29] However, the same value of pK_a was found in imidazole-containing ligands, such as cyclic dipeptides; e.g., *cyclo*-(glycyl-(*S*)-histidyl) ($pK_a = 6.25$) and *cyclo*-(*S*)-methionyl-(*S*)-histidyl) ($pK_a = 6.31$).[30] The second dissociation constant is clearly deduced to be phenol hydrogen, since this is the most basic site. The higher acid dissociation constant ($pK_{a2} = 9.67$) of the phenol group of tyrosine residue in HL4 compared with that of (*S*)-tyrosine ($pK_a = 9.04$)[29] may be due to a structural effect as a greater tendency towards a 15-membered hydrogen-bonded ring formation between the imidazole nitrogen of histidine and the phenol hydrogen of tyrosine residue (Fig. 8). The above result is consistent with that of cyclic voltammetry.

The potentiometric results for the acid dissociation constants of ligand HL4 are listed in Table 3, and the corresponding equilibria can be expressed as follows:

$$H_2L4^+ \rightleftharpoons H^+ + HL4 \qquad (2)$$

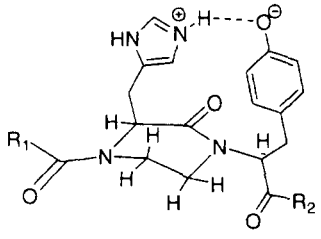

Fig. 8. Possible 15-membered ring of zwitter ion form of HL4.

Table 3. Acid Dissociation Constants of HL4 and Stability Constants of Cu^{2+} with HL4 at 25.0 °C and $\mu = 0.1$ mol dm^{-3}

Equilibrium quotient	Acid dissociation constants	Stability constants
$[H^+][HL4]/[H_2L4^+]$	$pK_{a1}=6.38$	
$[H^+][L4^-][HL4]$	$pK_{a2}=9.67$	
$[Cu(L4)^+]/[Cu^{2+}][L4^-]$		$\log K_1=7.16$
$[Cu(L4)_2]/[Cu(L4)^+][L4^-]$		$\log K_2=3.71$
Standard deviation (σ) [a]	0.01	0.04

a) In logarithm unit.

$$HL4 \rightleftharpoons H^+ + L4^- \quad (3)$$

On the other hand, the titration curve for 2 : 1 molar ratio of HL4 to Cu(II) ion has a long buffer region at low pH, and follows a weak inflection point at ca. $a = 1.5$—2.0, indicating that the complexation by $L4^-$ is essentially completed at this point, where a represents the moles of base added per mole of ligand present. During the course of titration, however, precipitations occurred at pH ≈ 6.9 and the insoluble species beyond pH ≈ 9.1 dissolved to produce a completely clear solution. Again, the equilibrium constants for the formation of 2 : 1 complex were calculated on the basis of Ref. 17. For this calculation, because of the formation of a solid phase in the pH region of $6.9 < pH < 9.1$, only the data at titration point $0 < a < 1.5$ (i.e., $4.2 < pH < 6.9$) were used. Thus, obtained the formation constants are listed in Table 3, and the corresponding equations are defined as given below:

$$Cu^{2+} + L4^- \rightleftharpoons Cu(L4)^+ \quad (4)$$

$$Cu(L4)^+ + L4^- \rightleftharpoons Cu(L4)_2 \quad (5)$$

The insolule species is probably due to the polymerizaiton product that is linked via phenolate anion and Cu^{2+} bridge, and/or due to the formation of copper(II) hydroxide.

Thermal Analyses. In order to distinguish between coordinated or hydrated water molecules, TGA and DTA of complexes **1** and **2** were measured. Both copper(II) complexes showed essentially the same thermal behavior. Figure 9 shows simultaneous TG and DTA curves for **2** as a typical example of the thermal analysis of copper(II) complexes. For the sake of convenience, each weight-loss (WL) step (which was monitored on the TG curve) is designated in Roman Numerals, and the corresponding peak temperature on the DTA curve is denoted as $T_{1max.}$, $T_{2max.}$, etc., in which the subscript (e.g., 1max) is the highest peak temperature that was observed in the first WL step. In addition, superscript s in the peak temperature shows whether the peak found in the same WL step is small or poor, or whether the peak is a shoulder. In the determined temperature ranges, the WL percentages in the mass and thermal effects accompanying the changes in the solid copper(II) complexes upon heating are summarized in Table 4.

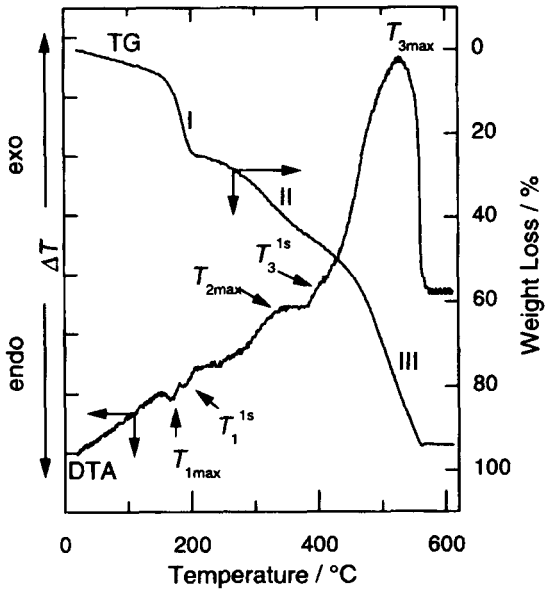

Fig. 9. TG and DTA curves for complex **2**.

For both copper(II) complexes, the TG and DTA curves showed that the thermal decomposition proceeded in several stages. The small endothermic peaks, which were observed in the first stages within the temperature range of 161—197 °C for **1** and 152—208 °C for **2**, could be correlated with

Table 4. Thermal Analysis Data for Cu(II) Complexes

Complex	Step num.	Temperature/°C		Weight loss/%	
		Range	Peak	Obsd (Calcd)	Effect type
1	I	161—197	T_{1max} = 173	23.1	Endo.
	II	389—549	T_{2max} = 441	93.1 (93.0[a])	Exo.
2	I	152—208	T_{1max} = 167	24.9	Endo.
			T_1^{1s} = 185		
	II	282—385	T_{2max} = 341	45.3	Exo.
	III	385—574	T_{3max} = 539	94.2 (92.9[a])	Exo.
			T_3^{1s} = 401		

a) Calcd as CuO.

the loss of coordinate and hydrated water. However, the observed WL values are not in accord with the calculated values (3.1% for **1** and 7.1% for **2**), and the latter percentage loss in mass is much higher than the former. This discrepancy might be explained by the hypothesis that the partial decomposition of the organic ligand took place together with the loss of coordinate and hydrated water molecules. For these reasons, we couldn't distinguish between coordinated and hydrated water molecules. At higher temperatures, exothermic peaks were observed for the copper(II) complexes which are due to decomposition and oxidation of the complexes. In addition, the detailed observation in both complexes revealed that there were small and broad exothermic peaks before the intense exothermic decomposition of the complexes. In conjunction with the TG and the DTA curves, in which no horizontal plateaus were found until decomposition was completed, it may be possible that the thermal decompositions take place gradually, and are accompanied by the elimination and decomposition of parts of the ligand and that no stable intermediates are formed during the thermal-decomposition process in each complex.

At temperature ranges higher than 550—570 °C, the DTA curves became quite horizontal, indicating that thermal decomposition was completed. Since the final WL values are in agreement with the calculated ones, the copper(II) complexes prepared in this study resulted in the formation of CuO, which was oxidized upon pyrolysis up to 650 °C.

Conclusion

The present study is aimed mainly at syntheses of model complexes with amino acid side chains only. Structurally constrained dipeptide eHY–OEt was efficiently prepared by a one-pot reaction. The copper(II) complexes are mononuclear square-pyramidal geometries with two nitrogen atoms of histidine imidazole, two oxygen atoms of tyrosine phenolate anion and external water as native GAO. UV-visible-NIR and CD spectra of the complex have the same characteristics as the inactive form of GAO. However, they are distinct from those of the active phenoxyl radical form.[31] Cyclic voltammetry also showed irreversible oxidation of phenol to phenoxyl radical at high potential. In order to isolate phenoxyl radical, substituent groups are required, such as native GAO, itself, or many model complexes.[4,7–9]

Although we reported didentate ligands with two or three amino acids, elimination of the ligand protection groups enables the synthesis of other large molecules, such as tridentate or tetradentate ligands, to bind the membrane and to connect the surface of a solid material, like silica gel. These can generate other functions to the peptides.

The authors are grateful to Ms. Rika Miyake of the Analytical Center, Graduate School of Science, Osaka City University, for measurement of elemental analyses and mass spectra. This study was supported in part by a Grant-in-Aid No. 08640719 from the Ministry of Education, Science, Sports and Culture.

References

1 a) D. Amaral, F. Kelly-Falcoz, and B. L. Horecker, *Methods Enzymol.*, **9**, 87 (1966). b) P. S. Tressel and D. J. Kosman, *Methods Enzymol.*, **89**, 163 (1982). c) H.-J. Krüger, *Angew. Chem., Int. Ed. Engl.*, **38**, 627 (1999).

2 a) N. Ito, S. E. V. Phillips, C. Stevens, Z. B. Ogel, M. J. Mcpherson, and P. F. Knowles, *Nature*, **350**, 87 (1991). b) N. Ito, S. E. V. Phillips, K. D. S. Yadav, and P. F. Knowles, *J. Mol. Biol.*, **238**, 794 (1994). c) N. Ito, P. F. Knowles, and S. E. V. Phillips, *Methods Enzymol.*, **258**, 235 (1995).

3 M. M. Whittaker and J. W. Whittaker, *J. Biol. Chem.*, **265**, 9610 (1990).

4 a) A. Sokolowski, H. Leutbecher, T. Weyhermuller, R. Schnepf, E. Bothe, E. Bill, P. Hildebrandt, and K. Wieghardt, *J. Biol. Inorg. Chem.*, **2**, 444 (1997). b) J. A. Halfen, B. A. Jazdzewski, S. Mahapatra, L. M. Berreau, E. C. Wilkinson, L. Que, Jr., and W. B. Tolman, *J. Am. Chem. Soc.*, **119**, 8217 (1997). c) M. A. Halcrow, L. M. Lindy Chia, J. E. Davies, X. Liu, L. J. Yellowlees, E. J. L. McInnes, and F. E. Mabbs, *Chem. Commun.*, **1998**, 2465.

5 a) U. Rajendran, R. Viswanathan, M. Palaniandavar, and M. Lakshminarayanan, *J. Chem. Soc., Dalton Trans.*, **1992**, 3563. b) H. Adams, N. A. Bailey, I. K. Campbell, D. E. Fenton, and Q.-Y. He, *J. Chem. Soc., Dalton Trans.*, **1996**, 2233.

6 a) M. M. Whittaker, W. R. Duncan, and J. W. Whittaker, *Inorg. Chem.*, **35**, 382 (1996). b) S. Itoh, S. Takayama, R. Arakawa, A. Furuta, M. Komatsu, A. Ishida, S. Takamuku, and S. Fukuzumi, *Inorg. Chem.*, **36**, 147 (1997).

7 a) J. A. Halfen, V. G. Young, Jr., and W. B. Tolman, *Angew. Chem., Int. Ed. Engl.*, **35**, 1687 (1996). b) Y. Wang and T. D. P. Stack, *J. Am. Chem. Soc.*, **118**, 1397 (1996). c) E. Saint-Aman, S. Ménage, J.-L. Pierre, E. Defrancq, and G. Gellon, *New J. Chem.*, **1998**, 393.

8 Y. D. Wang, J. L. DuBois, B. Hedman, K. O. Hodgson, and T. D. P. Stack, *Science*, **279**, 537 (1998).

9 a) P. Chaudhuri, M. Hess, U. Florke, and K. Wieghardt, *Angew. Chem., Int. Ed. Engl.*, **37**, 2217 (1998). b) P. Chaudhuri, M. Hess, T. Weyhermuller, and K. Wieghardt, *Angew. Chem., Int. Ed. Engl.*, **38**, 195 (1999).

10 a) Y. Kojima, *Trans. Met. Chem.*, **4**, 269 (1979). b) T. G. Fawcett, E. E. Bernarducci, K. Jespersen, and H. J. Schugar, *J. Am. Chem. Soc.*, **12**, 2598 (1980). c) J. P. Laussac, A. Robert, R. Haran, and B. Sarker, *Inorg. Chem.*, **25**, 2760 (1986).

11 a) T. Yamashita, H. Takenaka, and Y. Kojima, *Amino Acids*, **4**, 187 (1993). b) Y. Kojima and T. Yamashita, *Yuki Gosei Kagaku Kyokaishi*, **54**, 84 (1996).

12 Y. Kojima, M. Watanabe, Y. Seki, K. Yamato, and H. Miyake, *Chem. Lett.*, **1995**, 797.

13 K. A. Magnus, B. Hazes, H. Ton-That, C. Bonaventura, J. Bonaventura, and W. G. J. Hol, *Proteins*, **19**, 32 (1994).

14 J. A. Tainer, E. D. Getzoff, and D. C. Richardson, *Nature*, **36**, 284 (1983).

15 K. Yamato, H. Miyake, K. Hirotsu, and Y. Kojima, *Acta Crystallogr., Sect. C*, **C55**, 123 (1999).

16 In the cases of complexes **3** and **4**, insoluble species ware also obtained by warming for recrystallization.

17 A. J. Fry, "Laboratory Techniques in Electroanalytical Chemistry," ed by P. T. Kissinger and W. R. Heineman, Marcel Dekker Inc., New York, NY, USA (1996), Chap. 15, p. 469.

18 T. Moeller and R. Ferrius, *J. Inorg. Nucl. Chem.*, **20**, 261 (1961).

19 A. E. Martell and R. J. Motekaitis, "The Determination and Use of Stability Constants," VCH Publishers, New York, NY, USA (1988).

20 Y. Kojima, Y. Ikeda, E. Kumata, J. Maruo, A. Okamoto, K. Hirotsu, K. Shibata, and A. Ohsuka, *Int. J. Pept. Protein Res.*, **37**, 468 (1991).

21 B. J. Hathaway and D. E. Billing, *Coord. Chem. Rev.*, **5**, 143 (1970).

22 Y. Seki, H. Miyake, Y. Kojima, M. Doi, and S. Yano, *Mol. Cryst. Liq. Cryst.*, **276**, 79 (1996).

23 M. M. Whittaker and J. W. Whittaker, *J. Biol. Chem.*, **263**, 674 (1988).

24 We confirmed that this structure is stereochemically possible by CPK modeling and MM2 calculation (included in Chem 3D). "Chem 3D," CambridgeSoft Corp., Cambridge, MA, USA (1997), Ver. 4.0.

25 V. D. Parker, G. Sundholm, U. Svanholm, A. Ronlán, and O. Hammerich, in "Encyclopedia of Electrochemistry of the Elements Organic Section," ed by A. J. Bard and H. Lund, Marcel Dekker Inc., New York, NY, USA (1978), Vol. XI, p. 181.

26 a) G. A. Hamilton, P. K. Adolf, J. d. Jersey, G. C. DuBois, G. R. Dyrkacz, and R. D. Libby, *J. Am. Chem. Soc.*, **100**, 1899 (1978). b) M. Fontecave and J.-L. Pierre, *Bull. Soc. Chim. Fr.*, **133**, 653 (1996).

27 A. J. Baron, C. Stevens, C. Wilmot, K. D. Seneviratne, V. Blakeley, D. M. Dooley, S. E. V. Phillips, P. F. Knowles, and M. J. McPherson, *J. Biol. Chem.*, **269**, 2595 (1994).

28 S. Ménage, G. Gellon, J.-L. Pierre, D. Zurita, and E. Saint-Aman, *Bull. Soc. Chim. Fr.*, **134**, 785 (1997).

29 R. M. Smith and A. E. Martell, "Critical Stability Constants," Plenum Press, New York, NY, USA (1974), Vol. 1.

30 Y. Kojima, N. Ishio, and T. Yamashita, *Bull. Chem. Soc. Jpn.*, **58**, 759 (1985).

31 M. L. McGlashen, D. D. Eads, T. G. Spiro, and J. W. Whittaker, *J. Phys. Chem.*, **99**, 4918 (1995).